A tertiary interaction that links active-site domains to the 5′ splice site of a group II intron

Marc Boudvillain*†‡, Alexandre de Lencastre* & Anna Marie Pyle*‡

** Department of Biochemistry and Molecular Biophysics and ‡ Howard Hughes Medical Institute, Columbia University, New York, New York 10032, USA*
† Present address: Centre de Biophysique Moleculaire, CNRS, Rue Charles Sadron, 45071 Orleans, Cedex 2, France.

Group II introns are self-splicing RNAs that are commonly found in the genes of plants, fungi, yeast and bacteria[1,2]. Little is known about the tertiary structure of group II introns, which are among the largest natural ribozymes. The most conserved region of the intron is domain 5 (D5), which, together with domain 1 (D1), is required for all reactions catalysed by the intron[3]. Despite the importance of D5, its spatial relationship and tertiary contacts to other active-site constituents have remained obscure. Furthermore, D5 has never been placed directly at a site of catalysis by the intron. Here we show that a set of tertiary interactions (λ–λ′) links catalytically essential regions of D5 and D1, creating the framework for an active-site and anchoring it at the 5′ splice site. Highly conserved elements similar to components of the λ–λ′ interaction are found in the eukaryotic spliceosome.

To dissect the structure of the group II intron active site, we developed a strategy based on two new chemo-genetic approaches: nucleotide analogue interference mapping (NAIM) and nucleotide analogue interference suppression (NAIS)[4–9]. Using the NAIM strategy, we identified the nucleotides and atoms most important for group II intron function[5]. The NAIM results were then used as a guide for designing group II intron mutations in regions most likely to affect active-site function. Intron mutants were screened and characterized kinetically to evaluate the mechanistic role and importance of each mutated nucleotide. We used a *trans*-branching assay (Fig. 1a)[10] to explore the effects of mutations on trans-esterification and for optimizing conditions required for subsequent NAIS experiments[5]. For those mutants in which the branching reaction was strongly inhibited, we also conducted a 5′-splice-site hydrolysis assay[11,12] to obtain the D5 dissociation constant (K_d) and the chemical rate of reaction (k_{chem}). In this way, we could evaluate the specific mutational effects on interdomain binding or on chemical catalysis. Among the variety of mutations that strongly affected function of exD123 RNA (M.B. and A.M.P., unpublished data), those with pronounced effects on reaction chemistry were concentrated in a region near the 5′ end of D1 (represented by mutants exD123(G5:A) and exD123(A115:U), Table 1).

The partially functional exD123(G5:A) and exD123(A115:U) mutants and the *trans*-branching reaction (Fig. 1) were used in NAIS experiments designed to reveal tertiary contacts between the mutated residues and atoms in D5 (ref. 5). Disruption of energetic coupling between the position of mutation and a given functional

Table 1 Kinetic parameters of the exD123 mutants*

exD123	Branching† k_{obs} (10^{-4} min^{-1})	Hydrolysis k_{chem} (10^{-3} min^{-1})	K_d (μM)
Wild type	250 ± 10	87 ± 4	0.30 ± 0.04
G5:A	1.8 ± 0.2	8 ± 3	0.27 ± 0.09
A115:U	2.4 ± 0.1	2.7 ± 0.2	0.23 ± 0.09
A198:U‡	29 ± 2	52 ± 7	3.6 ± 0.9

* Branching and hydrolysis reactions were performed as described in Methods.
† For exD123(G5:A) and exD123(A115:U), the reaction end point could not be determined accurately and was assumed to be 0.44 as for wild-type exD123. For exD123(A198:U), the reaction end point is 0.12.
‡ A mutation that induces binding defects is presented for comparison: the A198→U mutation disrupts a ground-state hydrogen bond in the known ζ–ζ′ interaction between D1 and D5 (ref. 16), as inferred from the crystal structure of an analogous GNRA tetraloop-receptor complex[27]. The 10-fold increase in K_d corresponds to the loss of ~1.6 kcal mol^{-1} of D1–D5 interaction energy, which is consistent with the loss of at least one hydrogen bond.

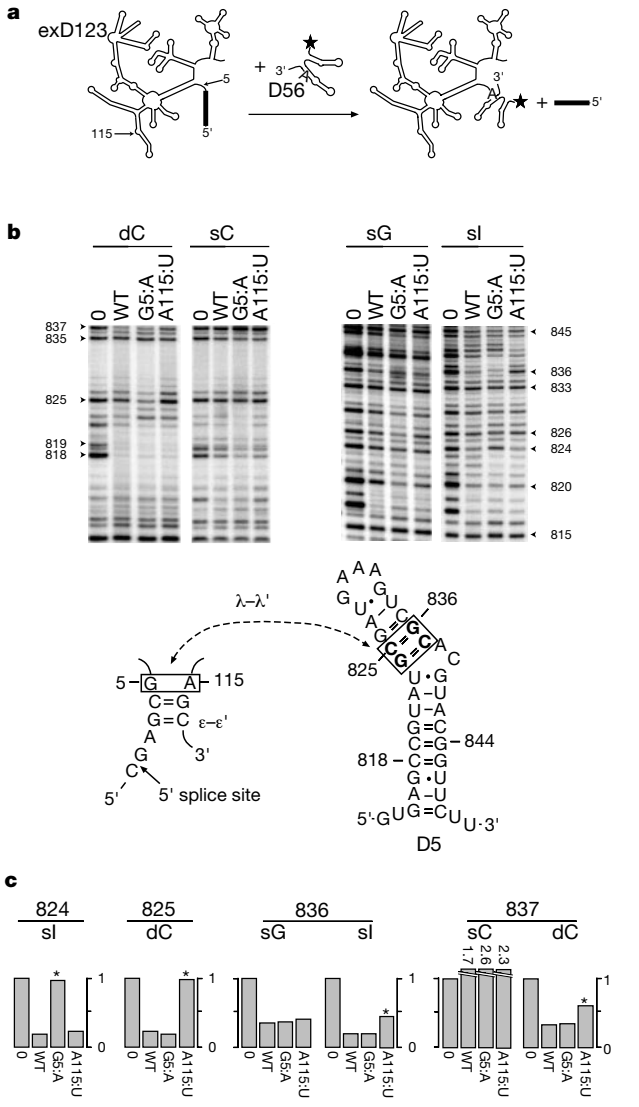

Figure 1 Nucleotide analogue interference suppressions within D5 and D1. **a**, The exD123 (5′ exon/domains 1–3) mutants were tested for changes in the D5 interference pattern using the *trans*-branching assay. Branching results in the chemical ligation of D56 and D123, thereby ensuring a simple selection of reacted molecules. **b**, To search for NAIS signals within D5, we reacted wild-type (WT) or mutant exD123 transcripts with 5′-^{32}P-labelled D56 transcribed with an array of NTPαS analogues. Autoradiographs correspond to iodine-cleaved transcripts modified with guanosine-αS (sG), cytosine-αS (sC), deoxy-C-αS (dC) or inosine-αS (sI). Band intensities were quantitated and corrected for background phosphorothioate effects as described[5]. **c**, Normalized intensities of bands corresponding to positions where NAIS signals were observed (indicated by an asterisk). The normalized intensities are mean values, each having a maximum variance of ± 20%, from 2–4 independent experiments. Unlike the lower-intensity background bands, the NAIS signals are reproducible, dependent on iodine-cleavage and mutant-specific (**b**), as described[5]. Comparative data are shown for NαS-containing D56 that were unreacted (0) or branched to wild-type exD123 (WT), exD123(G5:A) (G5:A) and exD123(A115:U) (A115:U) mutants. For suppressions at positions 824 and 825, significant phosphorothioate effects were not observed and so corresponding bars are not shown. The band intensity observed for unreacted material was arbitrarily fixed to one. For branched products, the size of the bars is related to 1/(interference effect); that is, the smaller the bar, the stronger the interference. The values of band intensities over 1 are shown above the corresponding bars.

group was revealed by suppression of an interference normally observed in D56 upon nucleotide analogue substitution (Fig. 1). The pattern of D56 interferences obtained with wild-type exD123 is similar to that previously described[5]; however, several differences were observed with the exD123(G5:A) and exD123(A115:U) mutants (Fig. 1). The G5→A mutation in D1 induces complete suppression of inosine interference at G824 in D5, whereas the A115 → U mutation suppresses deoxynucleotide interference at C825. In addition, the exD123(A115:U) mutant suppresses an inosine interference at G836 and partially rescues a strong deoxynucleotide interference at C837.

These results show energetic coupling between two nucleotides of D1 (G5 and A115) and two consecutive G·C pairs located at the base of D5 stem 2. This energetic coupling is likely to reflect specific interactions because the exD123(G5:A) and exD123(A115:U) mutants, which have similar reactivities (Table 1), yield NAIS signals that are not observed upon mutation of other positions in D1 or D3 (Fig. 1)[5]. The new interaction, which we have named λ–λ′, is composed of nucleotides that exhibit a high level of phylogenetic conservation and which show strong effects when mutated (M.B., A.D.L. and A.M.P., unpublished data).

Notably, the adjacent ϵ–ϵ′ interaction[13] brings G5 and A115 into close proximity (Fig. 1). The ϵ–ϵ′ motif contributes to 5′-splice-site selection[13], and it has also been observed that the ϵ-nucleotides G3 and C4 must be on the same molecule as their partners G116 and C117 for optimal chemical reactivity of ribozymes derived from the intron (S. Leuin and A.M.P., unpublished data). This suggests that ϵ–ϵ′ itself may be a component of the intron active-site. The λ–λ′ interaction therefore serves to join the ϵ–ϵ′ nucleotides in D1 with catalytically essential functionalities in D5 (refs 12, 14, 15), a role that is consistent with the fact that λ–λ′ mutations have marked effects on reaction chemistry (Table 1).

The λ–λ′ interaction is the third contact identified between D5 and another domain of the intron. The first contact identified (ζ–ζ′)[16] promotes D1–D5 association through a tetraloop–receptor interaction motif. Mutation of ζ–ζ′ functionalities induces binding defects in activity assays (Table 1)[12]. The κ–κ′ interaction also contributes primarily to the ground-state binding of D1 to D5 (M.B. and A.M.P., unpublished data). Consistent with this, both ζ–ζ′ and κ–κ′ involve atoms that lie on the so-called 'binding face' of D5 (refs 12, 15). Conversely, λ–λ′ involves D1 and D5 function-

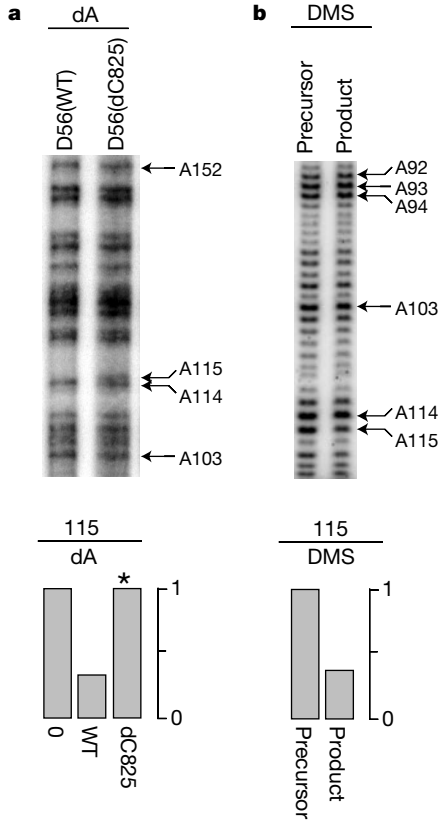

Figure 2 Single-atom NAIS and D5 interferences at A115. **a**, To search for NAIS signals within D1, we reacted wild-type exD123 transcripts containing NTPαS with 5′-^{32}P-labelled D56 molecules containing a single deoxynucleotide at C825 (D56(dC825)). The interference suppression observed for dA115 is specific, that is, it is not observed in the presence of other D56 modifications (such as dC837), and dC825 does not cause a suppression of dG5 interference (see Supplementary Information). Note that in these experiments, the 5′ exon was only 17 nucleotides in length (17D123, ref. 5). **b**, The involvement of A115 N1 is implicated by a D5-dependent DMS interference at position A115. Folded exD123 was reacted with DMS (1:100 dilution) for 5 min at room temperature. The DMS-modified exD123 was incubated with 3 μM D5 at 45 °C for 20 min under standard hydrolysis conditions[11]. Precursor exD123 was separated from the D123 product by PAGE, eluted and then primer extended using AMV reverse transcriptase for 15 min at 55 °C. After PAGE, products were analysed and quantitated on a PhosphorImager (Molecular Dynamics). The A115 interference value shown represents the average from three experiments, with a variance of 18%.

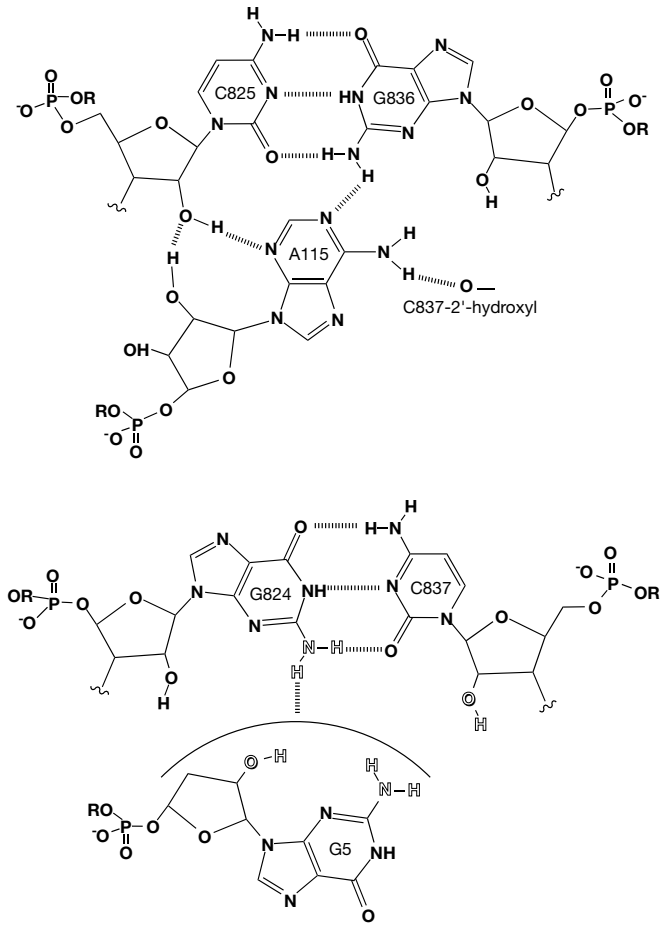

Figure 3 Model for the λ–λ′ interaction. Proposed arrangements of the two minor groove triples formed by A115 and G5 with the (5′-GC)·(5′-GC) tandem pairs in stem 2 of D5. Modelling (Insight II, Biosym/MSI) of the stacked triple interactions did not reveal any significant steric or geometric problems with the arrangements shown. Owing to a lack of constraints, the G824 amine is shown interacting with an undefined group on G5. Functionalities in this triple that have been implicated by NAIM experiments are shown in open lettering, indicating potential sites of interaction within the triple or with other nucleotides.

alities that have specific roles in catalysis (Table 1)[12]. It is therefore striking that the λ–λ′ interaction occurs on the previously defined 'chemical face' of D5 (refs 12, 15), where catalysis probably occurs.

All bonds in the proposed model for λ–λ′ involve atoms in the minor groove of both D5 and D1 components. The suppression data show that G5 interacts with N2 of G824, and that A115 interacts with N2 of G836 and the 2′-OH of C837 and C825. Previous work showed that G5 interacts through 2′-OH and N2 functionalities[5], whereas A115 interacts through a 2′-OH group[5]. Evidence for direct contact between the N1 of A115 and elements of D5 is provided by D5-dependent dimethyl sulphate (DMS) footprint[17] and interference signals at A115 (Fig. 2). Further evidence for a hydrogen bond between C825 and D1 was obtained through an adaptation of the single-atom NAIS approach[4–9], in which a chimaeric D56 molecule containing a single deoxynucleotide at C825 was reacted with exD123 transcripts modified with NTPαS. In that case, the specific suppression of a deoxynucleotide interference was observed at A115 (Fig. 2, and see Supplementary Information). The spatial arrangement that agrees best with this data is one in which the minor groove edge of A115 forms a triple interaction in the minor groove of the C825·G836 base pair (Fig. 3) using an arrangement that has been observed crystallographically[18]. G5 is likely to form a second minor groove triple with the G824·C837 base pair (Fig. 3). Because of the limited number of available constraints, this triple interaction is represented in a more general form.

On the basis of this information, the λ–λ′ interaction can be visualized as an extended minor-groove triplex that orientates the ϵ–ϵ′ helix along the 'chemical face' of D5, placing ϵ–ϵ′ against the D5 bulge (Fig. 4). A composite ϵ–ϵ′/λ–λ′ interaction that involves backbone–backbone interactions with the D5 bulge is inferred by strong deoxy and phosphorothioate interferences in ϵ–ϵ′ and the D5 bulge[5,12,19], as well as by evidence for metal ion binding in this region (J. Swisher, R. Sigel and A.M.P., unpublished data). A composite ϵ–ϵ′/λ–λ′ interaction (Fig. 4) would align the 5′ splice site next to major groove functionalities of G817 that have been shown to be critical for chemical catalysis by group II introns[15]. Thus, λ–λ′ is a novel substructure that links active-site constituents together and anchors them at a site of group II intron reaction.

The λ–λ′ interaction involves the fifth intronic nucleotide, which is invariably a guanine in group II introns[20] and in most nuclear introns[21]. In spliceosomal introns, G5 is part of a three-base-pair helix between the first several nucleotides of the intron and a section of U6 RNA called the 'ACAGA-box' (paired residues are underlined)[22,23], forming a duplex that may be analogous to the ϵ–ϵ′ interaction. It will be interesting to test whether this region interacts with a set of universally conserved G·C pairs in helix 2 of the U2–U6 complex, which has been proposed to be analogous to stem 2 of D5 (refs 19, 24, 25). The existence of such a spliceosomal λ–λ′ homologue might strengthen the hypothesis of an evolutionary relationship between active sites involved in nuclear pre-mRNA splicing and group II introns. □

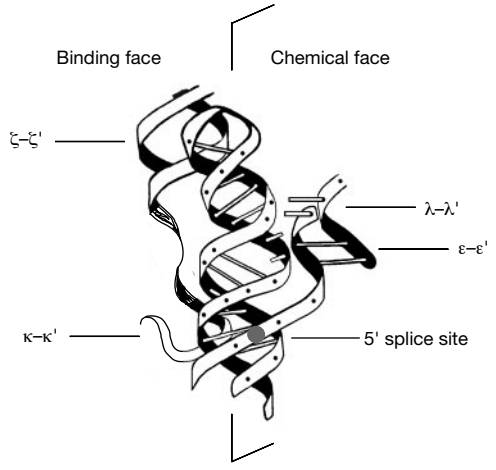

Figure 4 Representation of the putative group II intron active site, showing regions of D1 interacting with D5. On the left side of the model are the ζ–ζ′ and κ–κ′ contacts[5,16] between the D5 binding face[12] and the tetraloop receptor and three-way junction of D1. The right side of the model shows the D5 chemical face interacting with the extended λ–λ′/ϵ–ϵ′ interactions that align the 5′ splice site over the D5 catalytic locus[15].

Methods

Transcriptions

Plasmids encoding the mutant transcripts were prepared from precursor plasmid pJDI3′-673 (ref. 26) using the QuikChange site-directed mutagenesis kit (Stratagene) or according to described procedures[5]. Plasmids derived from pJDI3′-673 (encoding exD123 RNA) were linearized with *Bam*HI, pT7-D56 (encoding D56) with *Eco*RV (ref. 10) and pJDI5′-75 (encoding D5) with *Hpa*II (ref. 11) and transcribed as described[10,11]. Transcripts randomly modified with NTPαS analogues were prepared as described[5].

Reaction kinetics

Hydrolysis and *trans*-branching kinetic assays were carried out as described[10,11] with minor modifications. For branching kinetics, 5′-^{32}P end-labelled D56 transcripts (10 nM, final concentration) were mixed with exD123 (3 μM, final concentration) and heated at 95 °C for 1 min. We cooled the mixture to 42 °C and added salts (100 mM $MgCl_2$, 0.5 M NH_4Cl, 40 mM MOPS, pH 6) before further incubation at 42 °C. At various times, aliquots were withdrawn, quenched as described[5] and subjected to electrophoresis on stacked denaturing 4%:20% (top:bottom) polyacrylamide gels (PAGE). Hydrolysis kinetics were carried out similarly except that 5′-^{32}P end-labelled exD123 transcripts (1–5 nM, final concentration) were incubated with increasing concentrations of D5 (50 nM to 10 μM, final concentration) in 100 mM $MgCl_2$, 0.5 M KCl, 40 mM MOPS, pH 7.5 at 45 °C. Reactions were quantitated as described[11].

Nucleotide analogue interference suppression (NAIS)

We mixed wild-type exD123 (0.5 μM final concentration) and exD123 mutants (3 μM final concentration) with 5′-^{32}P end-labelled D56 transcripts (10 nM final concentration) that were randomly modified with a specific NTPαS analogue. The mixture was pre-incubated as described above and then reacted at 42 °C in 100 mM $MgCl_2$, 2 mM $Mn(AcO)_2$, 0.5 M $(NH_4)_2SO_4$, 40 mM MOPS, pH 6 (ref. 5). After 3 h of incubation at 42 °C, reaction products were resolved by PAGE. Iodine cleavage was performed as described[5], and the products were resolved by PAGE. Gel bands were quantitated using a phosphorimager (Molecular Dynamics) as described[5]. For single-atom NAIS, D56 molecules containing a deoxynucleotide at 825 (obtained by ligation of two synthetic oligonucleotides) were 5′-^{32}P end-labelled and were reacted with exD123 mutants (3 μM final concentration) randomly modified with NTPαS analogues under the conditions described above. Analysis of interferences in D1 was done as described[5].

Received 13 January; accepted 5 April 2000.

1. Michel, F. & Ferat, J.-L. Structure and activities of group II introns. *Annu. Rev. Biochem.* **64,** 435–461 (1995).
2. Pyle, A. M. in *Nucleic Acids and Molecular Biology* (eds Eckstein, F. & Lilley, D. M. J.) 75–107 (Springer, New York, 1996).
3. Qin, P. & Pyle, A. The architectural organization and mechanistic function of group II intron structural elements. *Curr. Opin. Struct. Biol.* **8,** 301–308 (1998).
4. Strobel, S. A. & Shetty, K. Defining the chemical groups essential for *Tetrahymena* group I intron function by nucleotide analog interference mapping. *Proc. Natl Acad. Sci. USA* **94,** 2903–2908 (1997).
5. Boudvillain, M. & Pyle, A. Defining functional groups, core structural features and inter-domain tertiary contacts essential fro group II intron self-splicing: a NAIM analysis. *EMBO J.* **17,** 7091–7104 (1998).
6. Ortoleva-Donnelly, L., Sweczak, A. A., Gutell, R. R., Strobel, S. A. The chemical basis of adenosine conservation through the *Tetrahymena* ribozyme. *RNA* **4,** 498–519 (1998).
7. Ortoleva-Donnelly, L., Kronman, M., Strobel, S. A. Identifying RNA minor grouve tertiary contacts by nucleotide analogue interference mapping with N2-methylguanosine. *Biochemistry* **37,** 12933–12942 (1998).
8. Strobel, S. A., Ortoleva-Donnelly, L., Ryder, S. P., Cate, J. H., Moncoeur, E. Complementary sets of noncanonical base pairs mediate RNA helix packing in the group I intron active site. *Nature Struct. Biol.* **5,** 60–65 (1998).
9. Szewczak, A., Ortoleva-Donnelly L., Ryder S. P., Moncoeur, E. & Strobel, S. A. A minor groove RNA triple helix within the catalytic core of a group I intron. *Nature Struct. Biol.* **5,** 1037–1042 (1998).
10. Chin, K. & Pyle, A. M. Branchpoint attack in group II introns is a highly reversible transesterification, providing a potential proofreading mechanism for 5′ splice site selection. *RNA* **1,** 391–406 (1995).
11. Pyle, A. M. & Green, J. B. Building a kinetic framework for group II intron ribozyme activity: quantitation of interdomain binding and reaction rate. *Biochemistry* **33,** 2716–2725 (1994).
12. Abramovitz, D. L., Friedman, R. A. & Pyle, A. M. Catalytic role of 2′-hydroxyl groups withing a group II intron active site. *Science* **271,** 1410–1413 (1996).
13. Jacquier, A. & Michel, F. Base-pairing interactions involving the 5′ and 3′ terminal nucleotides of

group II self-splicing introns. *J. Mol. Biol.* **213,** 437–447 (1990).
14. Peebles, C. L., Zhang, M., Perlman, P. S. & Franzen, J. F. Identification of a catalytically critical trnucleotide in domain 5 of a group II intron. *Proc. Natl Acad. Sci. USA* **92,** 4422–4426 (1995).
15. Konforti, B. B. *et al.* Ribozyme catalysis from the major groove of group II intron domain 5. *Mol. Cell* **1,** 1–20 (1998).
16. Costa, M. & Michel, F. Frequent use of the same tertiary motif by self-folding RNAs. *EMBO J.* **14,** 1276–1285 (1995).
17. Costa, M. & Michel, F. Tight binding of the 5′ exon to domain I of the group II self-splicing intron requires completion of the intron active sites. *EMBO J.* **18,** 1025–1037 (1999).
18. Pley, H. M., Flaherty, K. M. & McKay, D. B. Model for an RNA tertiary interaction from the structure of an intermolecular complex between a GAAA tetraloop and an RNA helix. *Nature* **372,** 111–113 (1994).
19. Chanfreau, G. & Jacquier, A. Catalytic site components common to both splicing steps of a group II intron. *Science* **266,** 1383–1387 (1994).
20. Michel, F., Umesono, K. & Ozeki, H. Compariative and functional anatomy of group II catalytic introns—a review. *Gene* **82,** 5–30 (1989).
21. Moore, M. J., Query, C. C. & Sharp, P. A. in *The RNA World* (eds Gesteland, R. F. & Atkins, J. F.) 303–358 (Cold Spring Harbor Laboratory Press, New York, 1993).
22. Kandels-Lewis, S. & Seraphin, B. Involvement of U6 snRNA in 5′ splice site selection. *Science* **262,** 2035–2039 (1993).
23. Lesser, C. F. & Guthrie, C. Mutations in U6 snRNA that alter splice site specificity: implications for the active site. *Science* **262,** 1982–1988 (1993).
24. Madhani, H. D. & Guthrie, C. A novel base-pairing interaction between U2 and U6 snRNAs suggests a mechanism for the catalytic activation of the splicesomes. *Cell* **71,** 803–817 (1992).
25. Yu, Y. T., Maroney, P. A., Darzynkiwicz, E. & Nilsen, T. W. U6 snRNA function in nuclear pre-mRNA splicing: a phosphorothioate interference analysis of the U6 phosphate backbone. *RNA* **1,** 46–54 (1995).
26. Jarrell, K. A., Dietrich, R. C. & Perlman, P. S. Group II intron domain 5 facilitates a trans-splicing reaction. *Mol. Cell. Biol.* **8,** 2361–2366 (1988).
27. Cate, J. H. *et al.* Crystal structure of a group I ribozyme domain: Principles of RNA packing. *Science* **273,** 1678–1685 (1996).

Supplementary information is available on *Nature*'s World-Wide Web site (http://www.nature.com) or as paper copy from the London editorial office of *Nature*.

Acknowledgements

We thank Q. Liu for preparing plasmids encoding exD123 mutants. We also thank S. Strobel for helpful discussions, R. Sousa for the clone of the Y639F RNA polymerase and P. S. Perlman for the gift of plasmids pJDI5′-75 and pJDI3′-673. M.B. is a Postdoctoral Research Associate and A.M.P. is an Assistant Investigator with the Howard Hughes Medical Institute, which we thank for financial support of this work. A.D.L. is supported by a fellowship from PRAXIS XXI (Portugal).

Correspondence and requests for material should be addressed to A.M.P. (e-mail: amp11@columbia.edu).

A ratchet-like inter-subunit reorganization of the ribosome during translocation

Joachim Frank*†‡ & Rajendra Kumar Agrawal†‡

** Howard Hughes Medical Institute, † Health Research Incorporated at the Wadsworth Center, and ‡ Department of Biomedical Sciences, State University of New York at Albany, Empire State Plaza, PO Box 509, Albany, New York 12201-0509, USA*

The ribosome is a macromolecular assembly that is responsible for protein biosynthesis following genetic instructions in all organisms. It is composed of two unequal subunits: the smaller subunit binds messenger RNA and the anticodon end of transfer RNAs, and helps to decode the mRNA; and the larger subunit interacts with the amino-acid-carrying end of tRNAs and catalyses the formation of the peptide bonds. After peptide-bond formation, elongation factor G (EF-G) binds to the ribosome, triggering the translocation of peptidyl-tRNA from its aminoacyl site to the peptidyl site, and movement of mRNA by one codon[1]. Here we analyse three-dimensional cryo-electron microscopy maps of the *Escherichia coli* 70S ribosome in various functional states, and show that both EF-G binding and subsequent GTP hydrolysis lead to ratchet-like rotations of the small 30S subunit relative to the large 50S subunit. Furthermore, our finding indicates a two-step mechanism of translocation: first, relative rotation of the subunits and opening of the mRNA channel following binding of GTP to EF-G; and second, advance of the mRNA/$(tRNA)_2$ complex in the direction of the rotation of the 30S subunit, following GTP hydrolysis.

We analysed the amplitude-corrected three-dimensional cryo-electron microscopy (3D cryo-EM) density maps of five complexes presenting the 70S ribosome in different functional states: (1) an initiation-state complex[2], bound with a mRNA and fMet–$tRNA_f^{Met}$ at the peptidyl (P) site (the 'control'); (2) the pre-translocational state complex[3], bound with mRNA, aminoacyl (A)- and P-site tRNAs, and EF-G in the presence of a nonhydrolysable GTP analogue, GMPP(CH_2)P (the 'GTP form'); (3) as (2), but without mRNA and tRNAs[3]; (4) the post-translocational state complex[3], bound with mRNA, P and exit (E)-site tRNAs, and EF-G in the presence of GTP and fusidic acid (the 'GDP form'); and (5) as (4), but without mRNA and tRNAs[3,4]. The comparison of these refined maps shows that, upon binding of EF-G/GMPP(CH_2)P to the ribosome, the 30S subunit rotates with respect to the 50S subunit by an angle of about 6 ($\pm$0.7) degrees, resulting in a maximum displacement, at the periphery of the ribosome, of 19 ($\pm$3) Å. The rotation is counterclockwise when seen from the solvent side of the 30S subunit (compare Fig. 1a and b). Following EF-G-dependent GTP hydrolysis, in the presence of fusidic acid the 30S subunit rotates back (Fig. 1c) by an angle of about 3 ($\pm$0.7) degrees. The conformational rearrangement is marked if one compares the distances between the L1-protein region of the 50S subunit and the platform and head regions of the 30S subunit (Fig. 1a and b). The positions of beak and spur of the 30S subunit are also strongly affected. Figure 1 shows maps of 70S/EF-G complexes lacking mRNA and tRNAs. The lower occupancy of EF-G/GMPP(CH_2)P in the complex containing tRNA at the A site[3,5] makes its presentation confusing, however the rotations of the subunit in the maps with or without mRNA and tRNAs are of the same size.

The rotation is accompanied by many conformational changes of the two subunits. Among these is a bifurcation of the stalk of the 50S subunit in the GTP state[3,5] (Fig. 1b) and its reversal to a single, elongated form in the GDP state[3–5] (Fig. 1c), showing an arc-like connection between the G′ domain of EF-G and the stalk base.

Going from the control to the GTP state, we also see a transition to a less compact structure[6], such that the radius of gyration increases[7] by 1.1 Å), and a complex rearrangement in the multi-stranded mass near the mRNA channel on the 30S subunit[8–11]. Significantly, both the entrance channel (conducting the downstream 3′ end of the mRNA) and the exit channel (conducting the upstream 5′ end of the mRNA) are affected (Fig. 2). The entrance channel is defined by a contact between the 30S subunit shoulder and head[12,13] involving the 530 loop, which is dynamic during decoding[14], and the 1050/1200 regions of the 16S rRNA[15], respectively. The entrance channel is much wider in both GTP (an increase in cross-sectional area by ~68%) and GDP (by ~118%) states than in the control (Fig. 3). Thus, the opening at the entrance site is wider (by ~30%) in the GDP (Figs 2b and 3c) than in the GTP (Figs 2a and 3b) state. The shape and position of the exit channel, formed between the platform and the head[11], are known to be variable[12,13]. The behaviour of this channel is the reverse of that of the entrance channel: it is wider in the GTP (Fig. 2c) than in the GDP state (Fig. 2d). Thus, a dynamic clamping mechanism apparently exists that alternatively secures the mRNA in the entrance channel or leaves it free to move following EF-G/GTP binding and GTP hydrolysis.

We find clear evidence in our cryo-maps that the positions of the tRNAs with respect to the 30S subunit are unchanged in the GTP state (Fig. 3b; ref. 16), indicating that translocation of the tRNA from the A to the P site has not taken place[3]. However, a contact

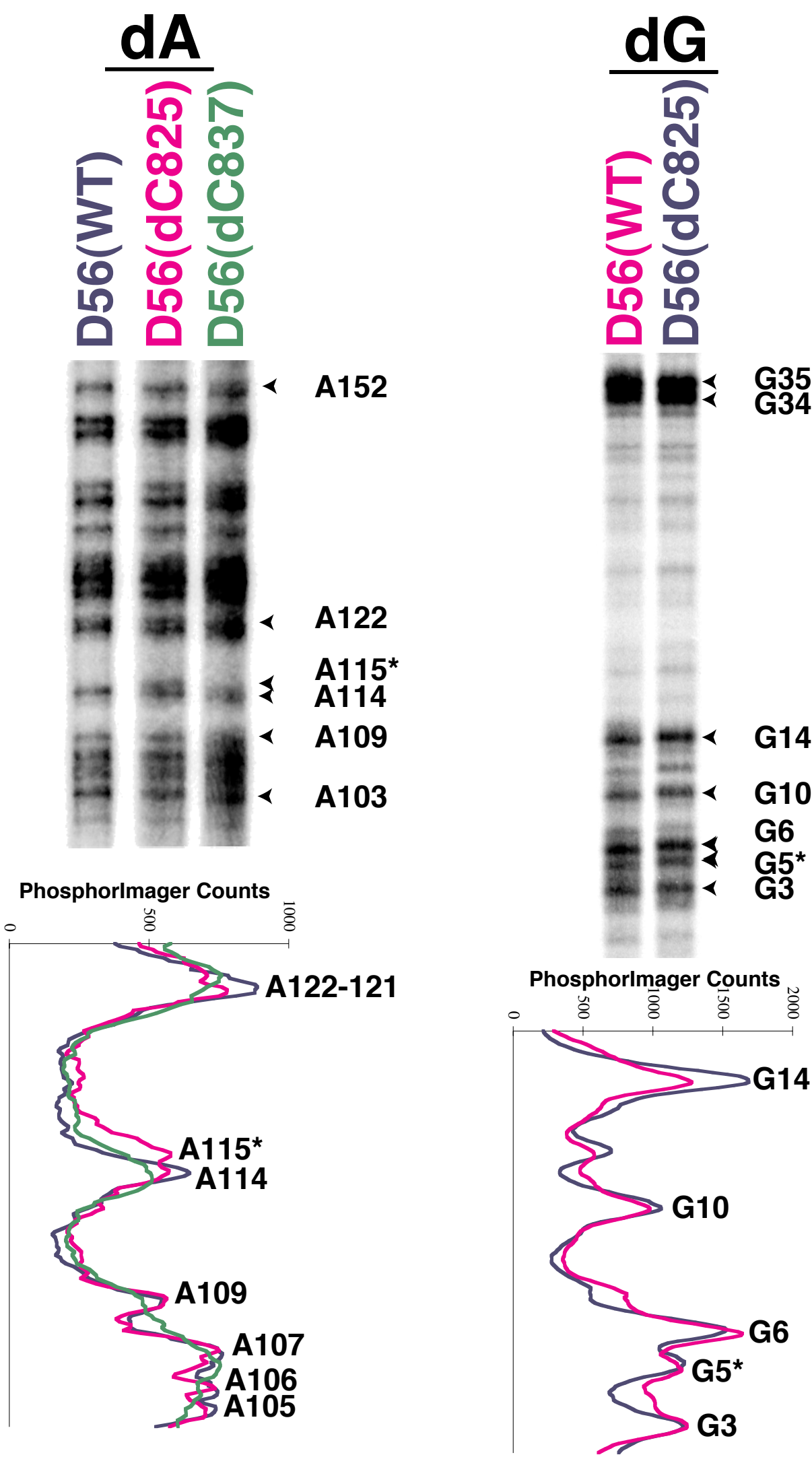
dA
D56(WT)
D56(dC825)
D56(dC837)
A152
A122
A115*
A114
A109
A103
PhosphorImager Counts
0
500
1000
A122-121
A115*
A114
A109
A107
A106
A105
dG
D56(WT)
D56(dC825)
G35
G34
G14
G10
G6
G5*
G3
PhosphorImager Counts
0
500
1000
1500
2000
G14
G10
G6
G5*
G3

Legend for supplementary figure: Single atom NAIS signals are specific. (Left:) Deoxynucleotide substitution at C837 does not suppress dA115 interference. Phosphorimager profile shows that dA115 interference (*) in WT (blue) is rescued by deoxynucleotide substitution at C825 (purple) but not by deoxynucleotide substitution at C837 (green). (Right:) Deoxynucleotide substitution at C825 does not suppress dG5 interference (*). PhosphorImager profile shows that dG5 interference in WT (purple) is unchanged by deoxy substitution at C825 (blue).